Theoretical Investigation of the Electronic Structure and Magnetic Properties in Ferromagnetic Rock-Salt and Zinc Blende Structures of 3d (V)-Doped MgS

ZEYNEB ABDELLI [1,2,3] ATHMANE MEDDOUR,[1] CHAHRAZED BOUROUIS,[1] and MOHAMMED HADI GOUS[1]

1.—Laboratoire de Physique des Matériaux, Université 8 Mai 1945 Guelma, BP 401, 24000 Guelma, Algeria. 2.—e-mail: abdelli.zeyneb@univ-guelma.dz. 3.—e-mail: zineb.abdelli.physique@gmail.com

In this work, we studied the properties of vanadium doped binary MgS compound $Mg_{1-x}V_xS$ (x = 0.125, 0.25, 0.50 and 0.75) in both ferromagnetic rock-salt and zinc-blende structures. The studied properties are structural, electronic and magnetic. The objective of this study is to explore the new dilute magnetic semiconductor systems. We have used two approximations to simulate these properties: Wu–Cohen generalized gradient approximation for structural properties, and the modified Becke–Johnson potential combined with the local density approximation for electronic and magnetic properties. The general context in which the calculations are done is based on the formalism of the spin-polarized density functional theory and the full-potential linear-augmented plane wave method. Among the various compounds studied, we have identified a ferromagnetic semiconducting behavior in the rock-salt structure. In the zinc-blende structure, we have one metallic candidate consisting of 75% V-doping of the Mg-sublattice, and all other compounds have a half-metallic ferromagnetic behavior. We conclude that the $Mg_{1-x}V_xS$ compounds, for x = 0.125, 0.25 and 0.50, in the zinc-blende structure are a diluted magnetic semi-conductors materials. To see the effects of the exchange splitting process, the exchange constants $N_{0\alpha}$ and $N_{0\beta}$ are calculated. For each concentration x, we have found the values of the total magnetic moment equal to 3 μ_β excepted for the case of $Mg_{0.25}V_{0.75}S$ compound in the zinc-blende structure. The value of the total magnetic moment is due principally to V magnetic atom and to other both nonmagnetic atoms Mg and S, which show small local magnetic moments localized on their sites. The presence of ferromagnetic order in this type of compound can be explained by the p-d hybridization phenomena.

Key words: MgVS, DFT calculations, FPLAPW, diluted magnetic semiconductors, spintronics, ferromagnetism, magnetic properties

INTRODUCTION

During the last decade, the exploration of new dilute magnetic semiconductors (DMS) designed for the development of practical semiconductor spintronics devices drew extensive attention worldwide.

As is known that the usefulness of semiconductors resides in the ability to dope them with

Theoretical Investigation of the Electronic Structure and Magnetic Properties in
Ferromagnetic Rock-Salt and Zinc Blende Structures of 3*d* (V)-Doped MgS

3795

impurities to engineer their band structures and improve their electronic performances.

In particular, transition metal (TM) doping usually induces magnetic properties into nonmagnetic semiconductors, so that both charge and spin degrees-of-freedom of the electrons must be taken into account simultaneously. This category of doped semiconductors with magnetic ground states is called diluted magnetic semiconductors (DMS).[1] DMS materials usually have special electronic properties, such as magneto-electronics, magneto-transport and they may play a key role in the future of science and technology.

Undoubtedly, if the DMS have the properties of half-metallic ferromagnets (HMF), they would find more suitable applications in spintronics. Half-metals are defined by electronic structures that exhibit simultaneously semiconducting or insulating, and metallic properties at the same time in materials, because of their electron spin orientations that are 100% polarized at the Fermi level.[2,3]

This phenomenon of half-metallic ferromagnetism was intensively explored in the past, and a complete spin polarization was not always observed. The experimental search for half-metals are generally tedious and verification of the expected spin polarization must be carried out. The density functional theory (DFT) has played an important role in this regard as it enables us to perform accurate electronic structure calculations.

Further exploration and predictive design based on the DFT method for a spintronic field can be achieved. Half-metallic properties of DMS compounds have been in fact studied using first-principle calculations. This type of research has especially focused on the transition metal doped III–V and II–VI three-dimensional (3D) semiconductors such as Mn and Cr doped GaN,[4,5] Fe doped CdS,[6] $Cd_{1-x}Cr_xZ$ (Z = S, Se and Te),[7] V doped CdS and CdTe.[8,9]

The search for possible spintronic materials has recently led to numerous studies on diluted magnetic semiconductors based on the alkaline earth oxides and alkaline earth chalcogenides as in Cr doped BeSe and BeTe,[10] Cr doped MgSe, MgTe and SrS [11,12] and V doped SrS, SrSe, SrTe and SrO.[13,14]

Magnesium sulfide (MgS) is among several classes of materials that are studied in this respect due to their unique properties. MgS is a wonderful barrier material for wide-gap quantum structures because of its large band gap of 4.5 eV. Moreover, it has other attractive features over the III–V semiconductors (e.g. GaN) such as a much larger exciton binding energies and, thus, is more suitable for applications in blue semiconducting lasers.[15]

The MgS binary compound exist in a two structures: in rock-salt (RS) with an indirect band gap[16,17] and in the zinc-blende (ZB) structure with a wide direct band gap (4.5 eV).[18] Furthermore, this compound exists in abundance in the earth's crust [19] and forms a very important closed-shell ionic system crystallizing in the NaCl structure at normal conditions. It is an important material in engineering with applications in diverse array of areas such as microelectronics, catalysis, medicine, spintronics, and optoelectronics.[15,20] MgS is still a matter of interest for theoretical and experimental physicists because of its promising properties.

Doping MgS with certain dopants may enhance its electronic, elastic, optical and magnetic properties. Currently, numerous studies have been conducted in order to investigate DMS based MgS properties by using experimental and theoretical methods.

The doping of transition metals on MgS has been studied and the results indicated that the electronic and magnetic properties are modified due to the impurity states.[21,22] Similarly, Gous et al.[21] demonstrate that the substitution of Mg by Cr atoms could tailor MgS to a ferromagnetic half-metal due to the effective p-d exchange. Recently, Chen et al.[23] reported that the properties of MgS can be tailored by the doping of Ce atom. Furthermore, it has been predicted that doping of TM such as Mn, Fe, Co and Ni in MgS are very promising approaches to achieve DMSs based on first-principles theoretical calculation.[22]

Although previous reports on MgS based DMS focused mainly on the behaviors of DMS based MgS by the doping of transition metal in the zinc-blende structure, the study on the doping of TM atoms in rock-salt MgS is rather rare. In this paper, we extend the magnetic study on ZB structure of MgS compounds to the more stable rock-salt structure.

Based on our knowledge, there are no experimental or theoretical works considering the effect of V on rock-salt MgS, and the V doped MgS in the zinc-blende phase.

In the present work, we present a comparative study of the influence of 3*d*-V substitutional doping at the Mg site with different concentrations on the structural, electronic and magnetic properties of MgS in both the ferromagnetic rock salt structure where our compounds are stable and the ZB structure, which is chosen for its great technological interest within the framework of first-principles calculations.

The remainder of the paper is organized into three other sections. "General Parameters" section contain some elements on DFT theory and the details of calculates which we have used in this work. In "Results and Discussion" section, we have presented all results, which we have obtained with some discussions related to the structural, electronic and magnetic properties of Mg-V-S compounds. Finally, we present the conclusion in "Conclusions" section.

GENERAL PARAMETERS

To get insight into the electronic structure of MgS doped with transition metal vanadium (V) impurity, the spin-polarized density functional theory

SPDFT[24] based calculations has been performed using the full-potential linearized augmented plane wave (FP-LAPW) method[25] as implemented in WIEN2K *ab initio* simulation code.[26] First, the generalized gradient approximation as parameterized in 2006 by Wu–Cohen (WC-GGA)[27] has been employed to describe the exchange and correlation energy-functional for the structure optimization. The latter provide an accurate account of solids with ground state structural properties.[24,28] In addition, we also apply the Tran-Blaha modified Becke–Johnson (TB-mBJ)[29] exchange potential combined with the local density approximation (LDA) approach for the corrected electronic structure and magnetic properties. The TB-mBJ functional theory known to be a successful method to estimate the band gap of the semiconductor. It yields very accurate band gap values and calculates band structure with high accuracy for wide gap insulators, sp-semiconductors and transition metal-based material.[29,30]

The space group of MgS in a rock-salt structure is Fm$\bar{3}$m (No. 225) where the Mg and S atoms occupies respectively (0, 0, 0) and (0.5, 0.5, 0.5) positions. On the other hand, in the zinc-blende structure, this compound has a F$\bar{4}$3m (No. 216) space group where the Mg and S atoms are situated, respectively, in (0, 0, 0) and (0.25, 0.25, 0.25) sites. Concerning the crystal structures of the ternary compound Mg$_{1-x}$V$_x$S, it is constructed from the unit cell of RS and ZB structures as a standard eight-atom supercell (Mg$_{1-x}$V$_x$S), which corresponds to (1*1*1) with cubic symmetry. In the unit cell of both RS and ZB structures, concerning the compounds with, respectively, 25% and 75% of V doping, we replace the Mg atoms at the vertex site of supercell and face-center sites with the V atoms and keeping the other three Mg atoms and the four S atoms unchanged. From this configuration, the cubic structure is obtained for the both structures with P$\bar{4}$3m (No. 215) space group for ZB and Pm$\bar{3}$m (No. 221) space group for RS. Meanwhile, for 50%, the crystal becomes a tetragonal structure with P$\bar{4}$m2 and P$\bar{4}$/mmm (No. 123) space groups for ZB and RS, respectively.

We constructed the (1*1*2) supercell of 16 atoms for $x = 0.125$ of the tetragonal structure with space group F43m (No. 216) and P4/mmm (No. 123) for ZB and RS, respectively.

In the present calculations the [Mg]: $3s^2\,2p^6$, [V]: $4s^2\,3d^3$ and [S]: $3s^2\,3p^2$ states behave as valence electrons for the Mg, V, and S, respectively. All energetically lower states are taken as semi-core and core states. The cutoff energy, which has been regarded as -6 Ry, defines the separation of valence and core states.

In order to achieve convergence for the energy eigenvalues, the wave functions in the interstitial region were expanded in the plane-wave with a cutoff of $R_{MT}K_{max} = 8$. Inside the muffin-tin

spheres, the valence wave functions were expanded up to $l_{max} = 10$. The magnitude of the largest vector in charge density Fourier expansion $G_{max} = 16(Ry)^{1/2}$ was chosen.

The muffin-tin sphere radii R_{MT} are regarded as 2, 2.27 and 2.2 atomic units (a.u.) for Mg, V and S, respectively.

Following the Monkhorst–Pack scheme,[31] the 14*14*14 mesh with 3000 points in the k-space was employed to perform integrations over the first Brillouin zone.

Self-consistency is assumed to be achieved when the total energy difference of the system is stable within 10^{-4} Ry and the electron charge density converged with an accuracy of 0.0001 e for the charge density distance between last two iterations of the self-consistent field (SCF) cycles. To obtain the correct results, all parameters of the calculations have been checked carefully.

RESULTS AND DISCUSSION

Structural Properties

The structural parameters such as the lattice parameter (α_0), the module of compressibility (B) and its derived first one (B') once optimized, are generally used in the calculation of the electronic, magnetic and other properties of solids.[25]

To look for the above-mentioned parameters for the case of the binary alloy MgS and its ternary alloys, we use the Birch–Murnaghan equation (1)[32] whose principle consists of fitting the latter with the curve of the total energy as a function of the volume.

$$E_{\text{Tot}}(V) = E_0(V) + \frac{B_0 V}{B'(B'-1)}\left[B\left(1 - \frac{V_0}{V}\right) + \left(\frac{V_0}{V}\right)^{B'} - 1\right] \tag{1}$$

From Table I, we remark that for MgS, our results of the lattice parameter (α_0) are in good agreement with the experimental data[33] and other theoretical results.[15–20,34–36] We recall that, for the ternary Mg$_{1-x}$V$_x$S alloys, no experimental or theoretical data were found in the literature to be compared with the present work.

The reduction of lattice constants with increasing V concentration in this case means that the ionic radius of V is smaller than the ionic radius of Mg atom.

The variation of the energy as a function of the volume of the Mg$_{1-x}$V$_x$S alloys when $x = 0$, 0.125, 0.25, 0.50, 0.75, 1 for ZB and RS structures in both the ferromagnetic and nonmagnetic phases were calculated to see which structure and which phase are the more stable. On the one hand, results exhibited in Fig. 1 display that the RS and ZB structures are more stable in the

Theoretical Investigation of the Electronic Structure and Magnetic Properties in Ferromagnetic Rock-Salt and Zinc Blende Structures of 3*d* (V)-Doped MgS

3797

Table I. Equilibrium lattice constant a_0, bulk modulus B and its pressure derivatives B′ for $Mg_{1-x}V_xS$ alloys obtained using the WC-GGA

Compounds	a_0 (Å)			B (GPa)	B′
	Present	Exp	Other		
RS structure					
MgS	5.189	5.19[43]	5.16[34], 5.18[35]	77.704	4.088
$Mg_{0.875}V_{0.125}S$	5.162			81.453	4.162
$Mg_{0.75}V_{0.25}S$	5.14			85.747	3.981
$Mg_{0.50}V_{0.50}S$	5.089			83.514	3.777
$Mg_{0.25}V_{0.75}S$	5.007			87.826	4.335
VS	4.874			65.710	6.530
ZB structure					
MgS	5.655	5.66[22]	5.64[35], 5.67[43]	57.771	4.086
$Mg_{0.875}V_{0.125}S$	5.616			59.203	4.183
$Mg_{0.75}V_{0.25}S$	5.609			61.608	4.232
$Mg_{0.50}V_{0.50}S$	5.537			69.772	3.977
$Mg_{0.25}V_{0.75}S$	5.443			58.820	4.032
VS	5.310		5.31[8]	87.555	3.102
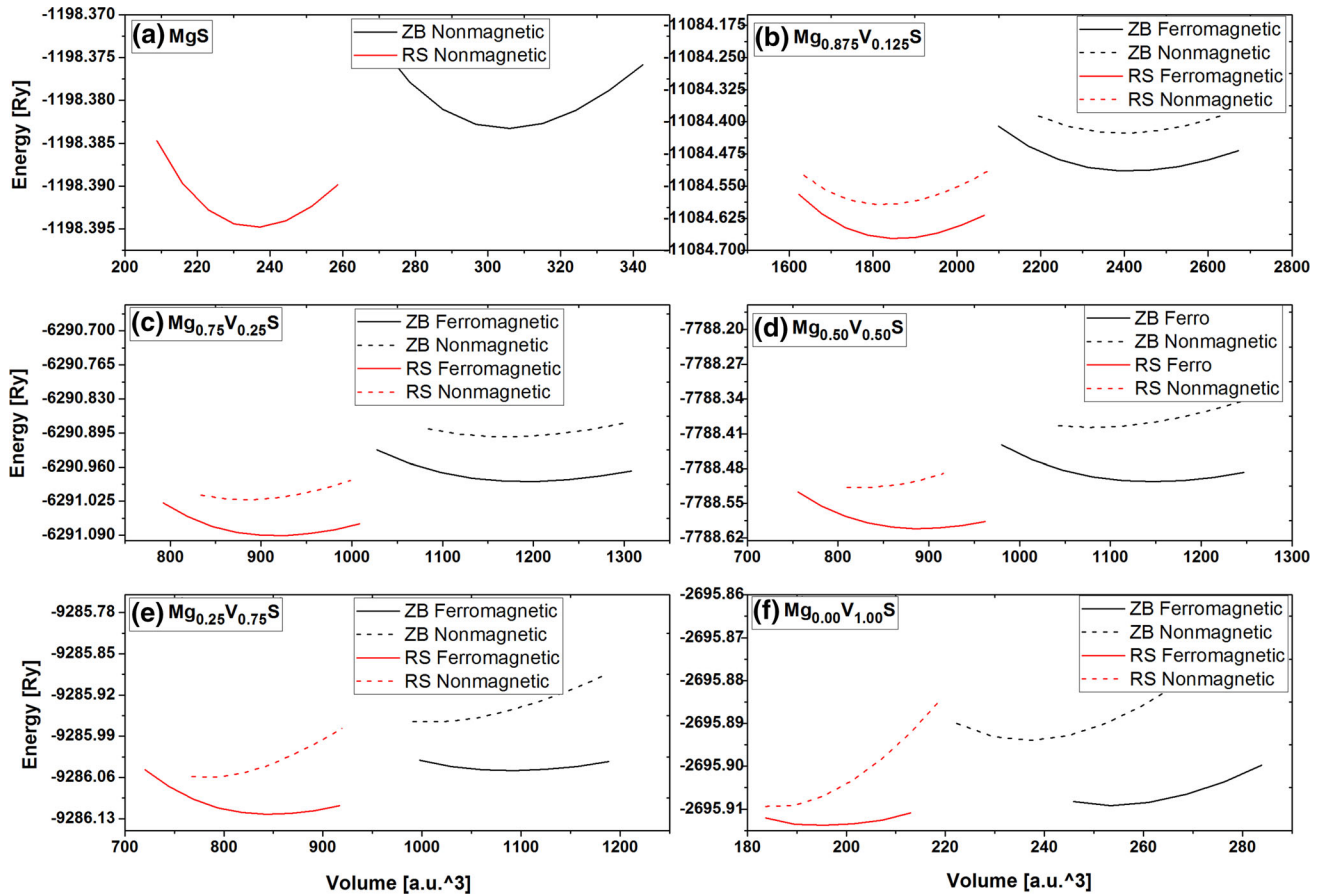
Fig. 1. Calculated total energy optimization as a function of volume per cell of (a) MgS, (b) $Mg_{0.875}V_{0.125}S$, (c) $Mg_{0.75}V_{0.25}S$, (d) $Mg_{0.50}V_{0.50}S$, (e) $Mg_{0.25}V_{0.75}S$ and (f) $Mg_{0.0}V_{1.0}S$ for ZB and RS phase in both nonmagnetic and ferromagnetic states. The red and black circles indicate the RS and ZB structures, respectively.

ferromagnetic phase, and on the other hand, we see that the ferromagnetic RS structure is more stable than the ferromagnetic ZB structure for all alloys.

From the obtained results on the stability of the binary MgS, we estimate that they are in good agreement, when we compared them with other theoretical results.[37,38]

Electronic Properties

Electronic Structure

The study of band structure is very important for any semiconducting material to determine its useful applications in optoelectronic, thermoelectric, magneto-optic and electromagnetic devices by calculation of energy band gaps. The electronic proprieties of MgS in both ZB and RS structures are available in the literature.[34,37] However, the influence of V impurities on the electronic properties of MgS semiconductor has not been investigated. The spin-polarized band structures of $Mg_{1-x}V_xS$ alloys (x = 0.125, 0.25, 0.50, 0.75) in both ZB and RS structure are calculated at their equilibrium lattice constants using the mbj-LDA along high symmetry directions of the first Brillouin zone (BZ) for both spin-up and spin-down cases are represented in Figs. 3, 4, 5, 6, 7, 8, 9 and 10, respectively. Therefore, we have plotted the band structure of the binary compound (MgS) for both structures, RS and ZB, in the nonmagnetic phase (Fig. 2). Table II contains the calculated values of energy gap (E_g) and half-metallic gap (G_{HM}) in both rock-salt and zinc-blende structures.

From Fig. 2, we see that MgS material is semiconducting with an indirect band gap located between Γ and X high-symmetry points for the RS phase and a direct band gap at Γ for the ZB phase. These results are in good agreement with other theoretical calculations.[34]

For the $Mg_{1-x}V_xS$ alloys (x = 0.125, 0.25, 0.50, 0.75), the analysis of band structures for a spin-down states found that the minima of the conduction band and the maxima of the valence band take place at the Γ point of the Brillion zone (see in Figs. 3, 4, 5, 6, 7, 8, 9 and 10). Where the Fermi level (E_F) lies in the middle of the VB maxima and the CB minima in all $Mg_{1-x}V_xS$ alloys for the RS structure, the concentrations x = 0.125, 0.25, 0.50 in the ZB structure thus present a semiconducting behavior in the spin-down channel. For the spin-up channel,
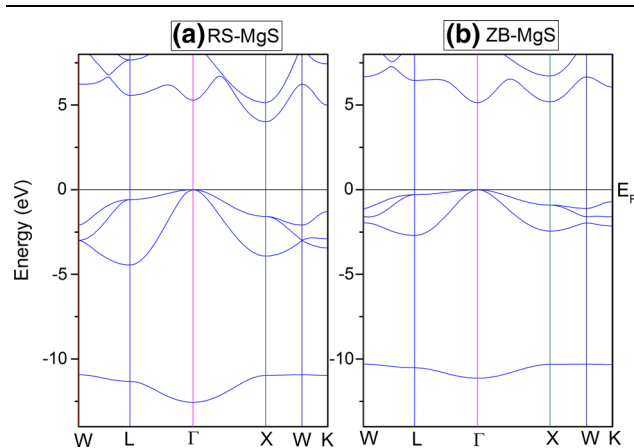
however, the E_F is situated in the upper part of the valence band maxima in the RS compounds structure, which possess a ferromagnetic semiconducting behavior for these alloys. However, in the case of the ZB structure, the VB maxima cross the E_F, which is a sign of a half-metallic character for the spin-down state; an exception is made for the $Mg_{0.25}V_{0.75}S$ compound, which has a metallic nature in both spin channels.

In our case, the half-metallic gap (G_{HM}) of all compounds is created between the conduction band minimum (CBM) and the Fermi level (0 eV), where the HM gap (G_{HM}) is defined as the minimum between the lowest energy of majority-spin and minority-spin conduction bands with respect to the Fermi level, and the absolute values of the highest energy of majority-spin and minority-spin valence bands,[39,40] which describes the minimal energy necessary to create a hole in the conduction bands of the minority spin. The values of energy gaps (E_g) and HM gap (G_{HM}) are given in Table II.

These results show that E_g decreases from x = 0 to 0.75 due to the widening of $3d$ (V) empty states in the gap of the minority-spin with increasing concentration (x) of vanadium. It should be noted that the values of E_g and G_{HM} given in Table II are for the spin-down configuration. The wide HM gap is a good sign of half-metallic ferromagnets.[13] Therefore, the $Mg_{0.875}V_{0.125}S$ with a higher HM gap (0.892 eV) in ZB structure is predicted to be a better potential candidate for exploring half-metallic ferromagnetic properties, and it will be used in the future as a semiconductor in spintronics applications.

Density of States

After the study of the electronic band structure of $Mg_{1-x}V_xS$ (x = 0, 0.125, 0.25, 0.50, 0.75) compounds, we have plotted the spin-polarized total densities of states (TDOS) and partial densities of states (PDOS) in order to consider their electronic structure in the ferromagnetic rock-salt and in the zinc-blende phase at their equilibrium lattice parameters. Our results for the contribution of each atom and orbital in different bands of the electronic band structure are shown in Figs. 11, 12, 13, 14, 15, 16, 17 and 18.

The non-symmetrical states are noted on the spin-up and spin-down TDOS curves. Their origin is due to the strong p-d hybridization between the $3p$ (S) and $3d$ (V) states at Fermi level E_F, seen in the spin-up direction. In RS structure, the hybridization is observed in the top of valence band, involving the states located lower than E_F. In the ZB structure, the hybridization is due to the states existing at E_F level giving the metallic nature for all $Mg_{1-x}V_xS$ compounds. On the other hand, for the minority-spin states, TDOS curves show a gap around the Fermi level for all concentrations of compounds in RS structure and for x = 0.125, 0.25, and 0.50 in ZB

Fig. 2. The band structure of the binary MgS (x = 0) in the nonmagnetic phase for both (a) RS and (b) ZB structures.

Theoretical Investigation of the Electronic Structure and Magnetic Properties in
Ferromagnetic Rock-Salt and Zinc Blende Structures of $3d$ (V)-Doped MgS

3799

Table II. Calculated results of the half-metallic G_{HM} (eV) band gaps, spin-minority band gaps E_g (eV), conduction band edge splitting (ΔE_C) and valance band edge splitting (ΔE_V) and exchange constants ($N_{0\alpha}$ and $N_{0\beta}$) of each site in $Mg_{1-x}V_xS$ alloys obtained using the mbj-LDA

Compounds	E_g (eV)	G_{HM} (eV)	ΔE_C (eV)	ΔE_v (eV)	$N_{0\alpha}$	$N_{0\beta}$	Material type
RS structure							
MgS	4.010	–	–	–	–	–	S
$Mg_{0.875}V_{0.125}S$	3.514	–	-0.037	-1.736	-0.200	-9.260	MS
$Mg_{0.75}V_{0.25}S$	3.370	–	-0.056	-1.825	-0.150	-4.860	MS
$Mg_{0.50}V_{0.50}S$	2.550	–	-0.397	-1.938	-0.530	-2.580	MS
$Mg_{0.25}V_{0.75}S$	2.160	–	-0.667	-2.120	-0.593	-1.884	MS
ZB structure							
MgS	5.130	–	–	–	–	–	S
$Mg_{0.875}V_{0.125}S$	4.844	0.892	1.102	-3.954	5.877	-21.14	HM
$Mg_{0.75}V_{0.25}S$	4.622	0.876	1.068	-4.359	2.848	-11.62	HM
$Mg_{0.50}V_{0.50}S$	4.581	0.610	1.468	-4.056	1.195	-5.409	HM
$Mg_{0.25}V_{0.75}S$	4.129	–	0.984	-4.585	0.875	-4.075	M

The last column shows the type of the material: *S* semiconductor, *MS* magnetic semiconductor, *HM* half-metal, *M* metal in both spin channels.
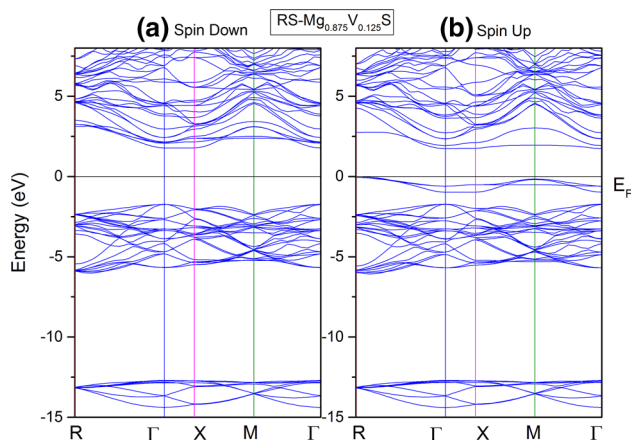
Fig. 3. Spin polarized band structures for $Mg_{0.875}V_{0.125}S$ in the RS structure, with (a) minority-spin (dn) and (b) majority-spin (up). The Fermi level is set to zero (horizontal line).
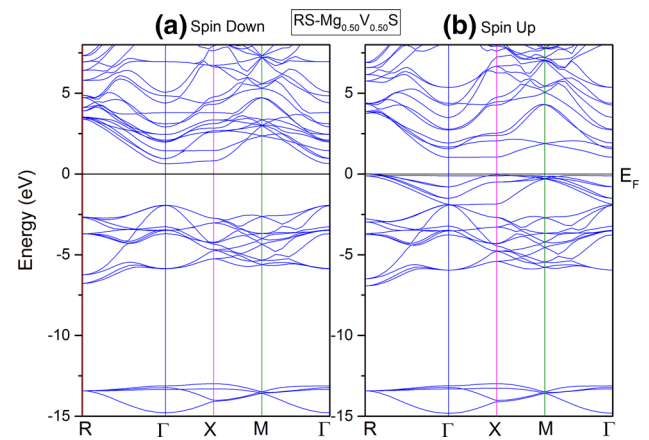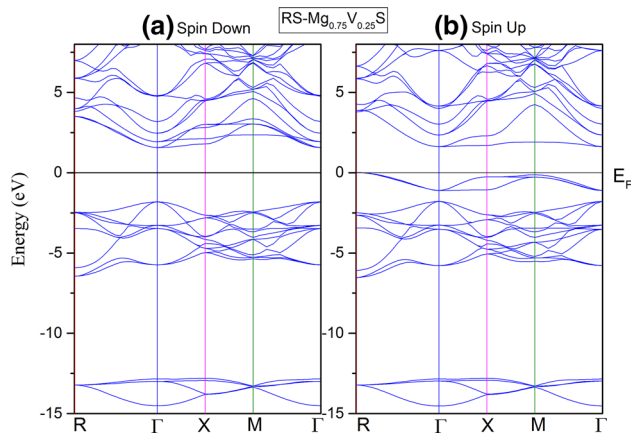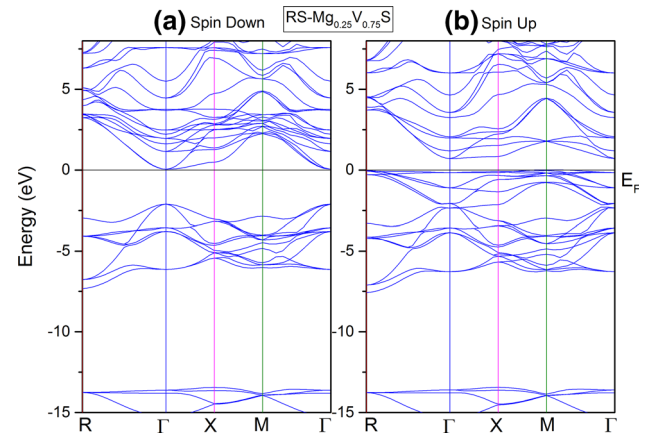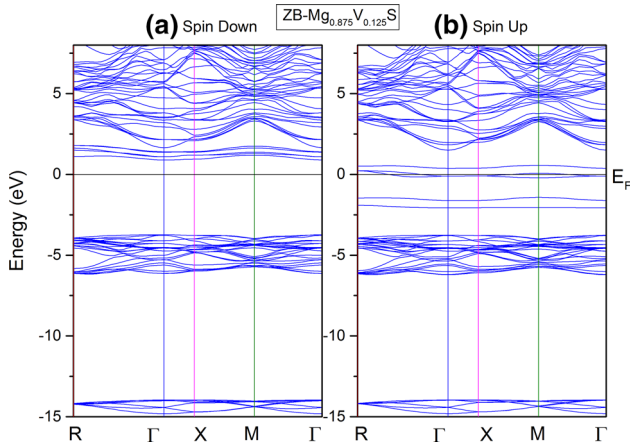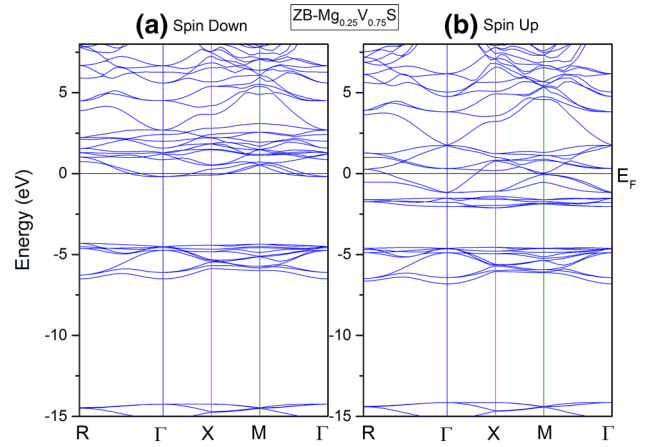

Fig. 5. Spin polarized band structures for $Mg_{0.50}V_{0.50}S$ in the RS structure, with (a) minority-spin (dn) and (b) majority-spin (up). The Fermi level is set to zero (horizontal line).

Fig. 4. Spin polarized band structures for $Mg_{0.75}V_{0.25}S$ in the RS structure, with (a) minority-spin (dn) and (b) majority-spin (up). The Fermi level is set to zero (horizontal line).
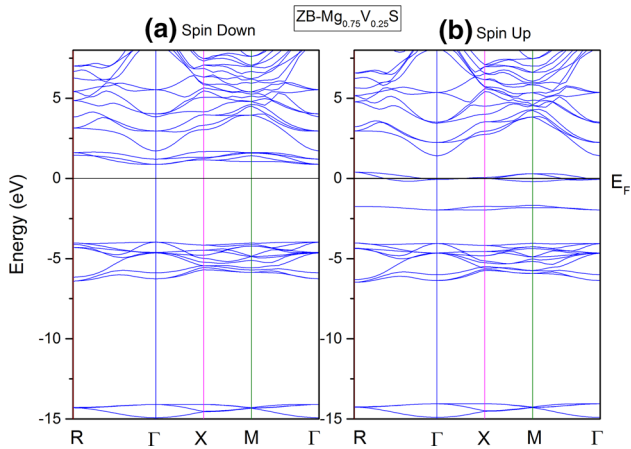

Fig. 6. Spin polarized band structures for $Mg_{0.25}V_{0.75}S$ in the RS structure, with (a) minority-spin (dn) and (b) majority-spin (up). The Fermi level is set to zero (horizontal line).

Fig. 7. Spin polarized band structures for $Mg_{0.875}V_{0.125}S$ in the ZB structure, with (a) minority-spin (dn) and (b) majority-spin (up). The Fermi level is set to zero (horizontal line).

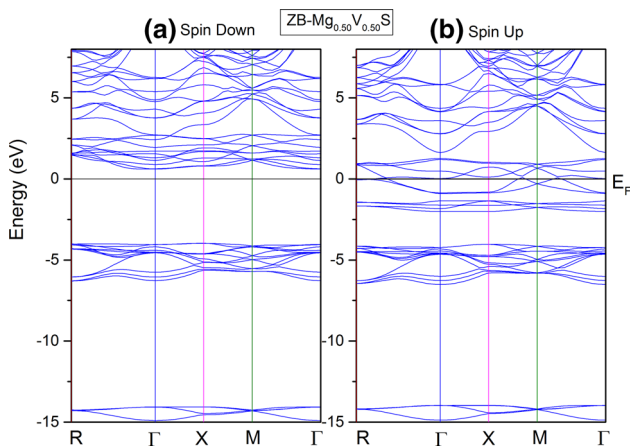Fig. 8. Spin polarized band structures for $Mg_{0.75}V_{0.25}S$ in the ZB structure, with (a) minority-spin (dn) and (b) majority-spin (up). The Fermi level is set to zero (horizontal line).

Fig. 9. Spin polarized band structures for $Mg_{0.50}V_{0.50}S$ in the ZB structure, with (a) minority-spin (dn) and (b) majority-spin (up). The Fermi level is set to zero (horizontal line).

Fig. 10. Spin polarized band structures for $Mg_{0.25}V_{0.75}S$ in the ZB structure, with (a) minority-spin (dn) and (b) majority-spin (up). The Fermi level is set to zero (horizontal line).

Fig. 11. Spin-polarized (a) total and (b) partial densities of states of $Mg_{0.875}V_{0.125}S$ in the RS structure. The Fermi level is set to zero (vertical dotted line).

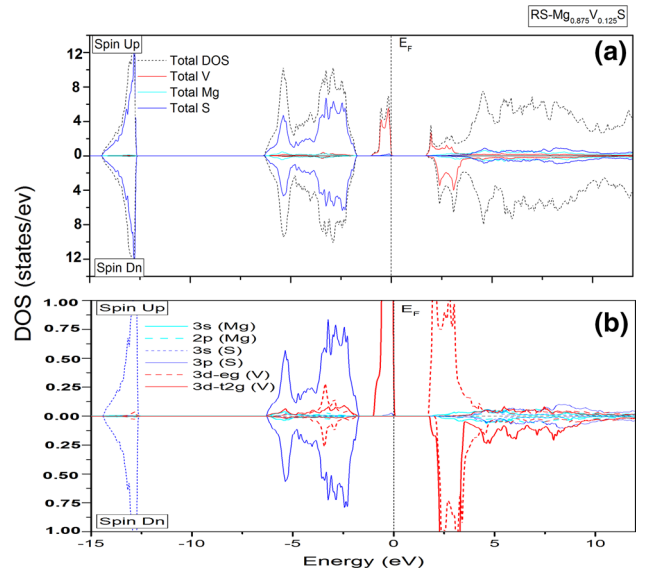structure. In summary, we can say that the studied compounds present the half-metallic ferromagnets behavior with a spin polarization of 100% at E_F in ZB structure and a ferromagnetic semiconductor behavior in the RS structure. Moreover, for $x = 0.75$ in ZB structure, the metallic nature is confirmed by the existence of an electronic state at the Fermi level in both spin channels.

The V^{2+} cation have the electronic configuration of [Ar] $3d^3$. It contributes two electrons to the host valence band semi-conductors, which contain $3p$ states of S. Correspondingly, to the crystal field theory and Hund's rule for each concentration, the PDOS show that the five-fold degenerate $3d$ (V) states, which are divided in two parts: the threefold degenerate low-lying $3d$ t_{2g} (dxy, dxz, and dyz) and the twofold generate high lying $3d$ e_g (dz^2, dx^2-dy^2) symmetry states. This is due to the effect of the octahedral crystal field formed by surrounding (S) ligands in RS where the valence configuration of the vanadium ion is V^{2+} ($4s^0 3d^3$-$t_{2g}^3 e_g^0$) having three
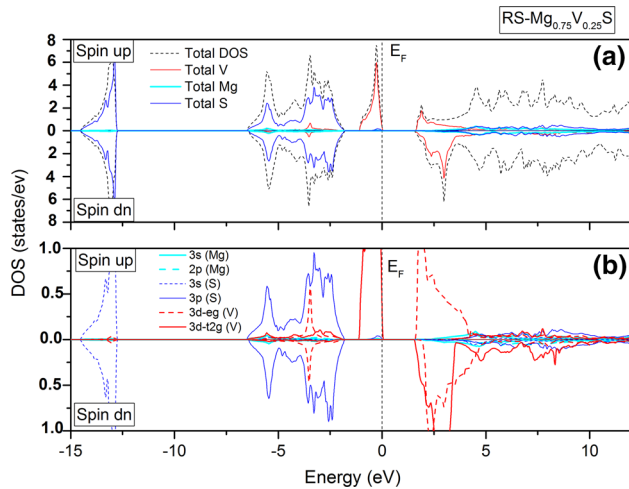
Fig. 12. Spin-polarized (a) total and (b) partial densities of states $Mg_{0.75}V_{0.25}S$ in the RS structure. The Fermi level is set to zero (vertical dotted line).

Fig. 13. Spin-polarized (a) total and (b) partial densities of states $Mg_{0.50}V_{0.50}S$ in the RS structure. The Fermi level is set to zero (vertical dotted line).
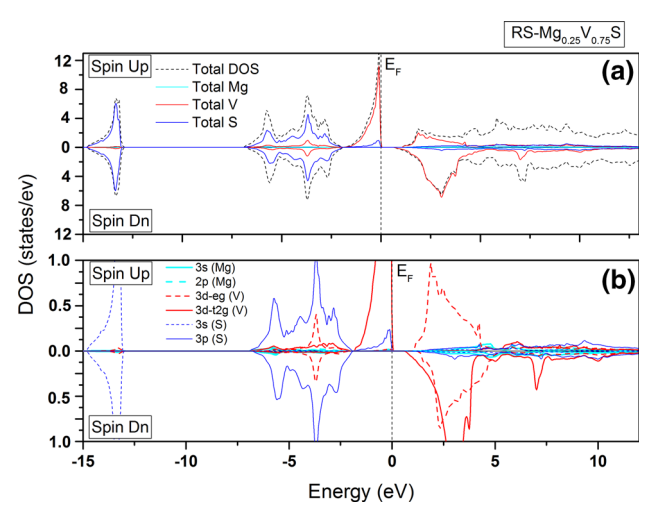

Fig. 14. Spin-polarized (a) total and (b) partial densities of states of $Mg_{0.25}V_{0.75}S$ in the RS structure. The Fermi level is set to zero (vertical dotted line).
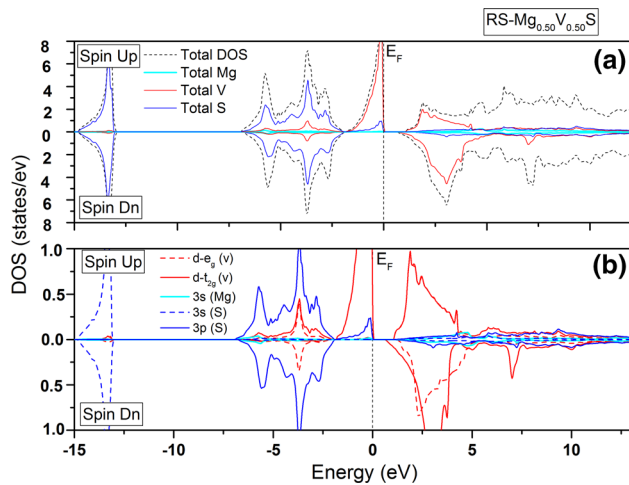

Fig. 15. Spin-polarized (a) total and (b) partial densities of states of $Mg_{0.875}V_{0.125}S$ in the ZB structure. The Fermi level is set to zero (vertical dotted line).

electrons in majority spin: three in t_{2g}^{3} (V) states and empty e_g^{0} (V) states.

Where in the ZB structure where the energy of $3d$ e_g states is lower than the energy of $3d$ t_{2g} states, the valence configuration of the vanadium ion is $3d^3$, with three electrons in majority spin, is the following: two in e_g^{2} (V) states and one electron in t_{2g}^{1} (V). This splitting of V-$3d$ states is due to the tetrahedral crystal field, formed by the surrounding S ion, letting the other minority spin states empty. It explains the origin of the main contribution to the calculated total magnetic moment value.

In the RS and ZB structures, the majority-spin states of the $Mg_{0.75}V_{0.25}S$ compound in the valence bands near E_F is due mainly to the t_{2g} (V) states with a very small contribution of the $3p$-S states; at the bottom of the conduction bands, the main contribution is due to the t_{2g} (V) states and $3p$ (S) states, whereas the hybridization between $3p$ (S)

and e_g (V) states is almost missing in the RS structure. It is known that the $3d$ (V) partially occupied states of Vanadium impurities are in the origin of created ferromagnetism in the $Mg_{1-x}V_xS$ systems. The $3p$-S states are centered in the valence band in the range between -6.45 (-6.43) eV and -1.74 (-3.67) eV for $Mg_{0.875}V_{0.125}S$, -6.62 (-6.46) eV and -1.76 (-3.67) eV for $Mg_{0.75}V_{0.25}S$, -6.85 (-6.51) eV and -1.90 (-4.06) eV for $Mg_{0.50}V_{0.50}S$ and -6.93 (-6.86) eV, and -1.92 (-4.47) eV for $Mg_{0.25}V_{0.75}S$ in RS (ZB) structure. In the highest part of the conduction band up to: 1.68 (1.77) eV, 1.57 (2.15) eV, 0.99 (2.77) eV and 0.92 (3.00) eV for $x = 0.125$, 0.25, 0.5 and 0.75, respectively, the DOS curves mainly constitute the $3p$-S states and $3s$-Mg with a week contribution of V-$3d$
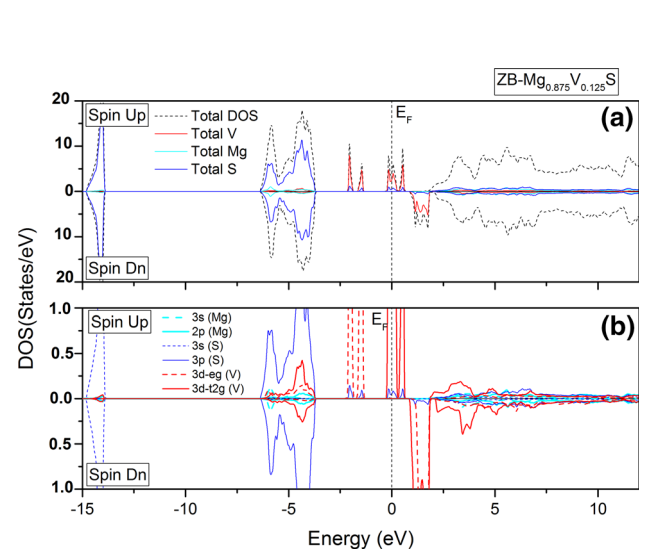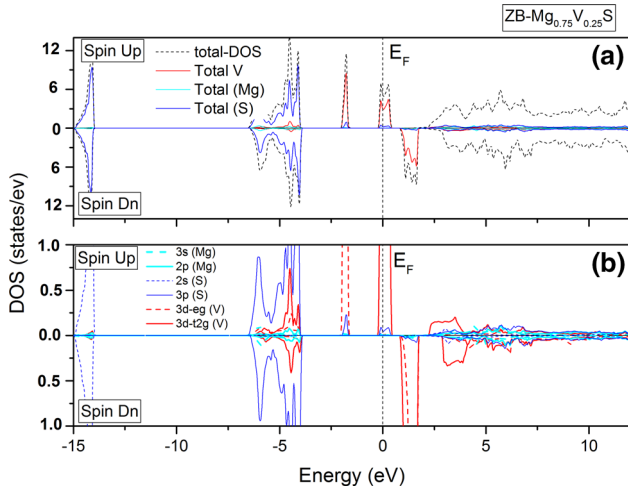
Fig. 16. Spin-polarized (a) total and (b) partial densities of states $Mg_{0.75}V_{0.25}S$ in the ZB structure. The Fermi level is set to zero (vertical dotted line).

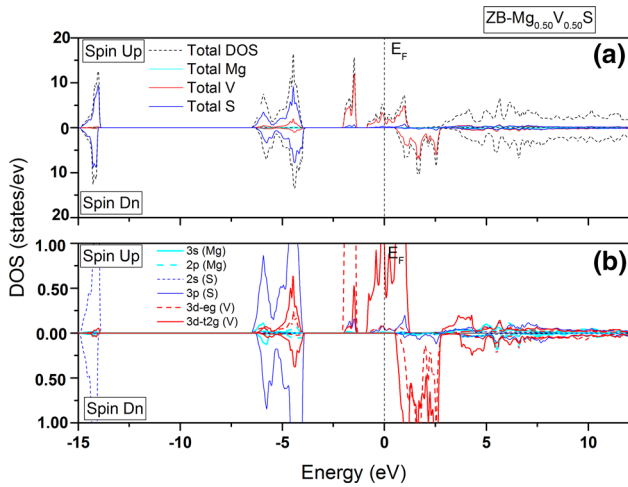Fig. 17. Spin-polarized (b) total and (b) partial densities of states of $Mg_{0.50}V_{0.50}S$ in the ZB structure. The Fermi level is set to zero (vertical dotted line).

Fig. 18. Spin-polarized (a) total and (b) partial densities of states $Mg_{0.25}V_{0.75}S$ in the ZB structure. The Fermi level is set to zero (vertical dotted line).

Table III. Calculated total and local magnetic moments (in μ_B) for $Mg_{1-x}V_xS$ in both RS and ZB structure using mbjLDA

Compounds	$V(\mu_B)$	$Mg(\mu_B)$	$S(\mu_B)$	$Tot(\mu_B)$
RS structure				
$Mg_{0.875}V_{0.125}S$	2.520	0.001	0.016	3.000
$Mg_{0.75}V_{0.25}S$	2.519	0.003	0.019	3.000
$Mg_{0.50}V_{0.50}S$	2.531	0.006	0.040	3.000
$Mg_{0.25}V_{0.75}S$	2.536	0.012	0.051	3.000
ZB structure				
$Mg_{0.875}V_{0.125}S$	2.344	0.008	$-$ 0.003	3.000
$Mg_{0.75}V_{0.25}S$	2.339	0.008	$-$ 0.007	3.000
$Mg_{0.50}V_{0.50}S$	2.336	0.017	$-$ 0.018	3.000
$Mg_{0.25}V_{0.75}S$	2.070	0.025	$-$ 0.009	2.593

in both cases. In the bottom of the valence band, it is the 3s-S states, which dominate.

Magnetic Properties

Exchange Coupling Constants

Based on the field theory, the expression of Hamiltonian is[41,42]:

$$H = -N_0 \beta s \cdot S \tag{2}$$

where N_0 and β are, respectively, cation content and expresses p-d exchange, s and S, represent, respectively, free hole and the V impurity spins. These parameters are used to calculate the total magnetic moment.

The $N_{0\alpha}$ and $N_{0\beta}$ values, which represent the exchange constant, are calculated according to
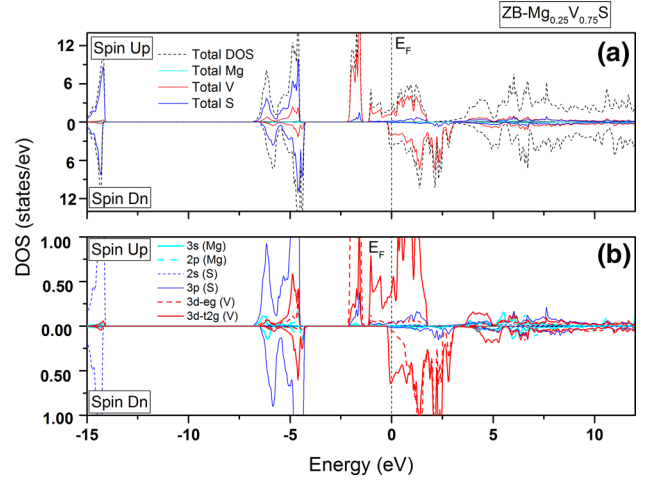
Eqs. 3 and 4 and it results, respectively, from s-d interaction in the conduction band and the p-d interaction in the valence band, respectively. These parameters can be calculated from the band structure and the magnetic properties by supposing the usual kondo interaction, which are known as[43]

$$N_{0\alpha} = \frac{\Delta E_c}{x \langle S \rangle} \tag{3}$$

$$N_{0\beta} = \frac{\Delta E_v}{x \langle S \rangle} \tag{4}$$

where ΔE_v and ΔE_c are the valence and conduction band edge splitting, respectively, estimated from the following equations:

$$\Delta E_c = E_{CBMin}^{\downarrow} - E_{CBMin}^{\uparrow} \tag{5}$$

$$\Delta E_v = E_{CBMax}^{\downarrow} - E_{CBMax}^{\uparrow} \tag{6}$$

x is the percentage of V in compound and $\langle S \rangle$ is the value of one-half of magnetization per V atom.

Theoretical Investigation of the Electronic Structure and Magnetic Properties in
Ferromagnetic Rock-Salt and Zinc Blende Structures of 3d (V)-Doped MgS
3803

Using mbj-LDA approximation, we have calculated ΔE_c, ΔE_v, $N_{0\alpha}$ and $N_{0\beta}$. Their values are listed in Table III. We observe that $N_{0\alpha}$ and $N_{0\beta}$ of the alloys decrease when the percentage of V increase confirming the magnetic character of these alloys.

The negative sign of both $N_{0\beta}$ and $N_{0\alpha}$ mean that the double-exchange mechanism exist in the RS structure compounds because the s-d and p-d interactions are parallel and give an FM character. The values of $N_{0\beta}$ in all compounds are more negative than $N_{0\alpha}$ meaning that the exchange energy involves through the spin-down channel. In the ZB structure, the negative signs of $N_{0\beta}$ and the positive signs of $N_{0\alpha}$ indicate, respectively, the antiferromagnetic exchange coupling between the valence band and the 3d states of V, and the ferromagnetic exchange coupling between the conduction band and valence band.

Magnetic Moment

The total magnetic moments M$_{\text{Tot}}$ of Mg$_{1-x}$V$_x$S alloys (x = 0.125, 0.25, 0.50 and 0.75) and atomic magnetic moments on Mg, V and S sites for both RS and ZB are calculated and listed in Table III. The obtained values show that total magnetic moment originates mainly from the atomic impurity V with a small contribution of Mg and S atoms.

We can also observe that the magnetic moment of the V atom is reduced. This change observed on V magnetic moment is created by the p-d hybridization between the V-3d and the S-p states. The reduced magnetic moment is shared between the nonmagnetic Mg and S sites. The atomic magnetic moments of V and S have opposite signs in the ZB structure, meaning that s-p states and V-3d states interact antiferromagnetically in the valence band.

CONCLUSIONS

We have presented a comparative study of the effect of vanadium doped magnesium sulfide (Mg$_{1-x}$V$_x$S) (x = 0.125, 0.25, 0.50 and 0.75) for both ferromagnetic rock-salt and zinc-blende structures by means of first-principles calculation using the Wien2k code.

The following are considered to be the most important findings of this work:

1. The structural properties results obtained using the WC-GGA approximation showed that the RS phase is more stable than ZB phase in all compounds.
2. The results of structural properties showed that the equilibrium lattice constant of Mg$_{1-x}$V$_x$S compounds decrease with increasing V concentration.
3. The electronic properties calculated using the equilibrium lattice parameters confirm that our compounds maintain a semiconducting nature for all of the Mg$_{1-x}$V$_x$S alloys (x = 0.125, 0.25, 0.50 and 0.75) in the RS structure and half-metallic character in the ZB structure, except for the Mg$_{0.25}$V$_{0.75}$S in ZB structure, which is of a metallic nature.
4. During the exchange splitting operation, the exchange constants $N_{0\alpha}$ and $N_{0\beta}$ values are in opposition signs. This confirms that there is opposite interaction between the valence and the conduction states in the ZB phase. However, in the RS phase the negative sign of both $N_{0\alpha}$ and $N_{0\beta}$ confirms the double-exchange mechanism caused by the s-d and p-d interactions. In all alloys, we have calculated a small local magnetic moment on the nonmagnetic Mg and S sites due to the hybridization between the V-3d and the S-3p states.

With regard to spintronics applications, V doped zinc-blende and rock-salt MgS systems show an interesting feature.

Finally, we can say that diluted magnetic semiconductors can be obtained in the MgS binary compound doped with a large range of concentrations of vanadium.

We think that the present study will can be open the way for future experimental work, especially in the spintronics field.

REFERENCES

1. I. Zutic, J. Fabian, and S. Das Sarma, *Rev. Mod. Phys.* 76, 323 (2004).
2. M.I. Katsnelson, V.Yu. Irkhin, L. Chioncel, A.I. Lichtenstein, and R.A. de Groot, *Rev. Mod. Phys.* 80, 315 (2008).
3. R.A. de Groot, F.M. Mueller, P.G. van Engen, and K.H.J. Buschow, *Phys. Rev. Lett.* 50, 2024 (1983).
4. Q. Zhao, Z. Xiong, L. Luo, Z. Sun, Z. Qin, L. Chen, and N. Wu, *J. Appl. Surf. Sci.* 396, 480 (2017).
5. A. Rani and R. Kumar, *J. Supercond. Nov. Magn.* 30, 1483 (2016).
6. Ch. Bourouis and A. Meddour, *J. Magn. Magn. Mater.* 324, 1040 (2012).
7. H.S. Saini, M. Singh, A.H. Reshak, and M.K. Kashyap, *J. Magn. Magn. Mater.* 331, 1 (2013).
8. H. Yahi, A. Meddour, and J. Magn, *Magn. Mater.* 401, 116 (2016).
9. M. Sajjad, H.X. Zhang, N.A. Noor, S.M. Alay-e-Abbas, A. Shaukat, and Q. Mahmood, *J. Magn. Magn. Mater.* 343, 177 (2013).
10. S.M. Alay-e-Abbas, K.M. Wong, N.A. Noor, A. Shaukat, and Y. Lei, *Solid State Sci.* 14, 1525 (2012).
11. N.A. Noor, S.M. Alay-e-Abbas, M.U. Sohaib, S.M. Ghulam Abbas, and A. Shaukat, *J. Magn. Magn. Mater.* 374, 164 (2015).
12. B. Doumi, A. Mokaddem, L. Temimi, N. Beldjoudi, M. Elkeurti, F. Dahmane, A. Sayede, A. Tadjer, and M. Ishak-Boushaki, *Eur. Phys. J. B* 88, 1 (2015).
13. B. Doumi, A. Mokaddem, F. Dahmane, A. Sayede, and A. Tadjer, *J. RSC Adv.* 5, 92328 (2015).
14. M. Berber, B. Doumi, A. Mokaddem, F. Dahmane, A. Sayede, and A. Tadjer, *J. Electron. Mater.* 47, 449 (2017).
15. R. Pandey and S. Sivaraman, *J. Phys. Chem. Solids* 52, 211 (1991).
16. A.L. Ruoff, T. Li, A.C. Ho, M.F. Pai, H. Luo, R.G. Greene, C. Narayana, J.C. Molstad, S.S. Trail, F.J. DiSalvo, and P.E. van Camp, *Phys. Rev. Lett.* 81, 2723 (1998).
17. S.M. Peiris, A.J. Campbell, and D.L. Heinz, *J. Phys. Chem. Solids* 55, 413 (1994).
18. M. Cardona and G. Harbeke, *Phys. Rev. A* 137, 1467 (1965).

19. M. Wang, X. Li, M. Gao, H. Pan, and Y. Liu, *J. Alloys Compd.* 603, 158 (2014).
20. M.W. Wang, M.C. Phillips, J.F. Swenberg, E.T. Yu, J.O. McCaldin, and T.C. McGill, *J. Appl. Phys.* 73, 4660 (1993).
21. M.H. Gous, A. Meddour, and Ch. Bourouis, *J. Supercond. Nov. Magn.* 29, 2849 (2016).
22. M.H. Gous, A. Meddour, and Ch. Bourouis, *J. Magn. Magn. Mater.* 422, 271 (2017).
23. Z.J. Chen, X.T. Zu, Y.X. Wang, and S.W. Xue, *J. Appl. Phys.* 105, 063532 (2009).
24. S.M. Alay-e-abbas, N. Sabir, Y. Saeed, and A. Shaukat, *Int. J. Mod. Phys. B* 25, 3911 (2011).
25. K.M. Wong, S.M. Alay-e-Abbas, A. Shaukat, Y. Fang, and Y. Lei, *J. Appl. Phys.* 113, 014304 (2013).
26. P. Blaha, K. Schwarz, G.K.H. Madsen, D. Kvasnicka, and J. Luitz, WIEN2K, an Augmented Plane Wave + Local Orbitals Program for Calculating Crystal Properties. Universität, Austria (2014).
27. Z. Wu and R.E. Cohen, *Phys. Rev. B* 73, 235116 (2006).
28. S.M. Alay-e-Abbas, S. Nazir, K. MunWong, A. Shaukat, and U. Schwingenschlögl, *EPL Europhys. Lett.* 106, 27003 (2014).
29. F. Tran and P. Blaha, *Phys. Rev. Lett.* 102, 226401 (2009).
30. Q. Mahmood, M. Hassan, and N.A. Noor, *J. Phys.: Condens. Matter* 28, 506001 (2016).
31. H.J. Monkhorst and J.D. Park, *Phys. Rev. B* 13, 5188 (1976).
32. F.D. Murnaghan, *Proc. Natl. Acad. Sci. U.S.A.* 30, 244 (1944).
33. L. Konczenwicz, P. Bigenwald, T. Cloitre, M. Chibane, R. Ricou, P. Testud, O. Briot, and R.L. Aulombard, *J. Cryst. Growth* 159, 117 (1996).
34. G. Kalpana, B. Palanivel, R.M. Thomas, and M. Rajagopalan, *Phys. Rev. B* 222, 223 (1996).
35. S. Duman, S. Bagcı, H.M. Tutuncu, and G.P. Srivastava, *Phys. Rev. B* 73, 205201 (2006).
36. A. Lichanot, A. Dargelos, C. Larrie, and R. Orlando, *Solid State Commun.* 90, 189 (1994).
37. F. Drief, A. Tadjer, D. Mesri, and H. Aourag, *J. Catal. Today* 89, 343 (2004).
38. G. Gokoglu, M. Durandurdu, and O. Gulseren, *Comput. Mater. Sci.* 47, 593 (2009).
39. K.L. Yao, G.Y. Gao, Z.L. Liu, and L. Zhu, *Solid State Commun.* 133, 301 (2005).
40. G.Y. Gao, K.L. Yao, E. Şaşioğlu, L.M. Sandratskii, Z.L. Liu, and J.L. Jiang, *Phys. Rev. B* 75, 174442 (2007).
41. Y. Huang, W. Jie, and G. Zha, *J. Alloys Compd.* 555, 117 (2013).
42. G.A. Gaj, R. Planel, and G. Fishman, *Solid State Commun* 29, 435 (1979).
43. S. Sanvito, P. Ordejon, and N.A. Hill, *Phys. Rev. B* 63, 165206 (2001).
44. Q. Mahmood, G. Murtaza, R. Ahmad, T. Hussain, and I.G. Will, *J. Curr. App. Phys.* 16, 361 (2016).